nature neuroscience

Coherent gamma oscillations couple the amygdala and striatum during learning

Andrei T Popescu, Daniela Popa & Denis Paré

The basolateral amygdala (BLA) mediates the facilitating effects of emotions on memory. The BLA's enhancing influence extends to various types of memories, including striatal-dependent habit formation. To shed light on the underlying mechanisms, we carried out unit and local field potential (LFP) recordings in BLA, striatum, auditory cortex and intralaminar thalamus in cats trained on a stimulus-response task in which the presentation of one of two tones predicted reward delivery. The coherence of BLA, but not of cortical or thalamic, LFPs was highest with striatal gamma activity, and intra-BLA muscimol infusions selectively reduced striatal gamma power. Moreover, coupling of BLA-striatal unit activity increased when LFP gamma power was augmented. Early in training, the rewarded and unrewarded tones elicited a modest increase in coherent BLA-striatal gamma. As learning progressed, this gamma coupling selectively increased in relation to the rewarded tone. Thus, coherent gamma oscillations coordinate amygdalostriatal interactions during learning and might facilitate synaptic plasticity.

Emotional arousal generally enhances memory[1], and much data suggest that the BLA is responsible for this effect[2]. Emotionally arousing events and their anticipation cause increases in the firing rate of BLA neurons[3,4]. Pharmacological interventions that interfere with this enhanced BLA activity decrease memory for events that took place shortly before the interference in many learning tasks[5]. On the inhibitory avoidance task, for example, intra-BLA infusions of GABA agonists[6] or glutamate receptor antagonists[7] just after training reduce long-term recall measured days later, well after the effects of these drugs have dissipated. Conversely, drugs that presumably enhance BLA activity such as bicuculline[8] and agonists of beta-adrenergic[9] and muscarinic[10] receptors enhance recall when injected within 2 h of training, but do not when injected later.

In contrast with Pavlovian cued fear learning[11,12], the above effects do not depend on storage in the BLA, but instead depend on storage in other structures that receive BLA inputs. For example, post-learning intra-BLA infusion of amphetamine increases striatal-dependent storage of response information and hippocampal-dependent storage of spatial information. In contrast, infusing lidocaine in the BLA shortly before testing long-term recall has no effect on either task[13]. Overall, these findings imply that the BLA facilitates memory consolidation in other brain structures during emotional arousal. This effect extends to various types of memories, including types of motor learning that depend on striatal plasticity.

Consistent with this, we have shown that BLA inputs can facilitate induction of corticostriatal long-term potentiation (LTP)[14]. However, because these experiments involved the delivery of electrical stimuli *in vitro*, the manner in which the amygdala and striatum interact during learning *in vivo* remains unclear. We addressed this question by carrying out extracellular recordings of unit activity and LFPs in basal amygdaloid nuclei, striatum, auditory cortex and intralaminar thalamic nuclei during the acquisition of a stimulus-response task that is known to depend on striatal plasticity[15].

RESULTS

Correlated amygdalostriatal activity in the waking state

We recorded unit activity and LFPs in six cats using high-impedance tungsten microelectrodes (see Methods). All striatal recordings were obtained in a ventral sector of the putamen adjacent to the amygdala, where neostriatal projections of the cat BLA are densest[16]. Histological controls (**Supplementary Fig. 1** online) indicated that our sample of extracellularly recorded cells included 139 striatal, 159 cortical, 55 thalamic intralaminar and 152 BLA neurons. Analyses of firing rates and spike durations (**Supplementary Fig. 2** online) revealed that $\geq$70% of the neurons in each structure fell into one dominant cell class. These neurons presumably correspond to principal striatal (medium spiny), cortical (pyramidal or stellate), thalamic (relay) or BLA (pyramidal) neurons. The following analyses are restricted to these dominant classes of neurons.

In search of a possible physiological signature of amygdalostriatal interactions, we first analyzed the coherence spectra of simultaneously recorded BLA and striatal LFPs during epochs of spontaneous waking (**Fig. 1a**). This analysis revealed that except for frequencies below 3 Hz, coherence of BLA and striatal LFPs was maximal in the gamma range (35–45 Hz). To test if this property also applied to other major striatal inputs, we carried out the same analysis between striatal and cortical (**Fig. 1b**) or between striatal and thalamic (**Fig. 1c**) LFPs. Although all combinations of recording sites showed coherent low-frequency

Center for Molecular & Behavioral Neuroscience, Rutgers State University, Newark, New Jersey, USA. Correspondence should be addressed to D. Paré (pare@andromeda.rutgers.edu).

Received 11 December 2008; accepted 26 February 2009; published online 10 May 2009; doi:10.1038/nn.2305

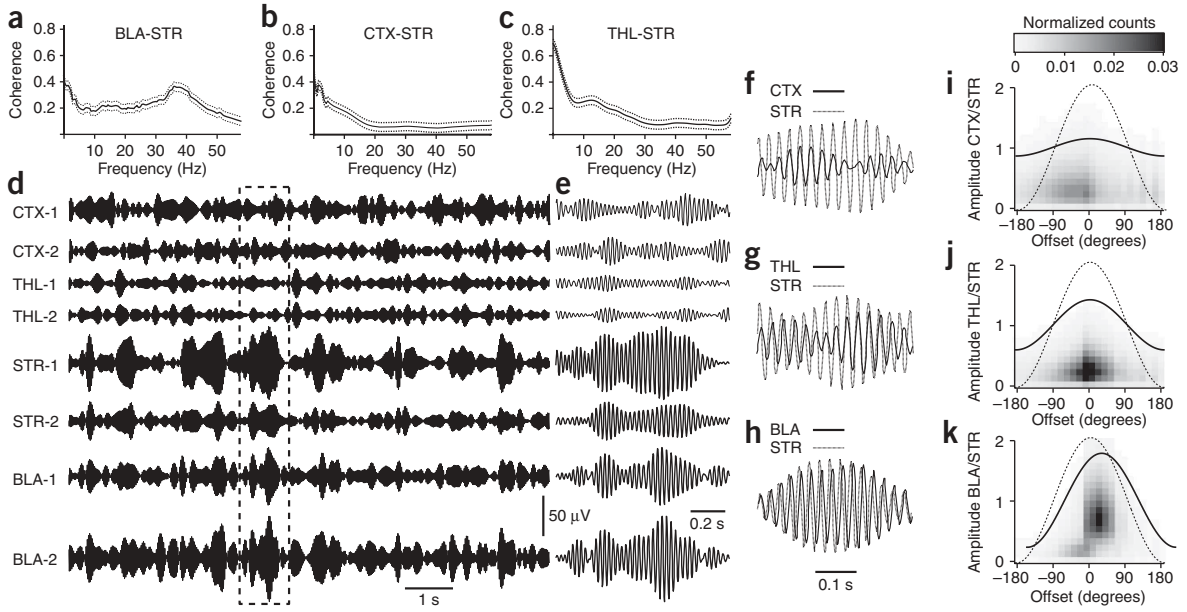

Figure 1 Coherent gamma activity in the BLA and ventral striatum during wakefulness. (**a**–**c**) Coherence ± s.e.m. versus frequency for all available pairs of simultaneous LFP recordings in the BLA and striatum (STR, $n = 696$; **a**), auditory cortex (CTX) and striatum ($n = 572$; **b**), and intralaminar thalamus (THL) and striatum ($n = 304$; **c**). (**d**,**e**) LFPs simultaneously recorded at the sites listed above and digitally filtered to isolate gamma (35–45 Hz) with a slow (**d**) and fast (**e**) time scale. Examples of two cortical (primary, top; associative, bottom), thalamic (anterior, top; posterior, bottom), striatal and BLA sites are shown. Dashed rectangle in **d** marks the segment expanded in **e**. (**f**–**h**) A brief period of high-amplitude striatal gamma (thin line) superimposed with cortical (**f**), thalamic (**g**) and BLA (**h**) gamma (thick lines). (**i**–**k**) Normalized frequency distributions (color coded) of phase lags between striatal versus cortical (**i**), thalamic (**j**) or BLA (**k**) gamma (*x* axis) as a function of normalized gamma amplitude (*y* axis). The lines overlaid on these graphs represent the average gamma cycles seen at the corresponding sites.

activity, the coherence of gamma oscillations was much higher between striatal and BLA LFPs ($F_{2,3,819} = 1{,}255.64$, $P < 0.0001$). In contrast, the coherence of BLA and thalamic or cortical gamma was low (**Supplementary Fig. 3** online).

Notably, the same weak relationship was seen between striatal gamma versus cortical or thalamic gamma whether we separately considered primary or associative auditory areas as well as posterior or anterior intralaminar thalamic nuclei (**Fig. 1d**). Visual inspection of these signals confirmed the preferential coupling of striatal gamma to BLA activity, relative to thalamic and cortical fast oscillations. One possible explanation for this result could be that BLA recording sites are physically closer to the striatum than thalamic or cortical recording sites. At odds with this possibility, however, the same results were obtained when we separately considered BLA, cortical, and thalamic recording sites that were equidistant from the striatum (**Supplementary Fig. 4** online).

Next, we obtained quantitative estimates of the phase relationship between striatal gamma versus cortical, thalamic or BLA gamma (**Fig. 1e**–**h**). To this end, we identified striatal gamma cycles of high amplitude ($\geq$2.5 s.d. of average) and measured the interval between the peak of the striatal gamma cycles versus the other sites. Although average phase lags were similar at all recording sites, they were much more variable at cortical (**Fig. 1i**) and thalamic (**Fig. 1j**) sites than in the BLA (**Fig. 1k**). The significance of this difference was assessed by computing an ANOVA on the cycle-to-cycle deviations from the average phase lag for the three combinations of recording sites ($F_{2,7,317} = 1{,}526.5$, $P < 0.0001$). A similarly variable phase relationship was seen between BLA and cortical or thalamic gamma (**Supplementary Fig. 5** online). There was an average 40 ± 14–degree phase shift between BLA and striatal gamma. We observed no relationship between the distance separating the BLA and striatal recording sites and phase lags ($r = 0.001$; **Supplementary Fig. 6** online).

To determine whether the coherent gamma activity seen in the BLA and striatum resulted from the influence of a common input or if the BLA contributed to generate gamma activity in the striatum, we compared the effects of bilateral intra-BLA infusions of the same volume (1 µl per hemisphere) of saline ($n = 4$) or muscimol ($n = 5$, 4 nM in saline) on striatal LFP power (**Fig. 2**). It should be noted that the volume of the cat BLA is much higher than in rats, with the cat basolateral nucleus spanning more than 4 mm in the dorsoventral axis, as compared with 1 mm in rats. Thus, to expose as many BLA neurons to muscimol as possible while minimizing mechanical distortion of the tissue and muscimol diffusion outside BLA, the total injected volume (1 µl per hemisphere) was divided in ten 0.1-µl infusion sites separated by 0.2 mm along a single dorsoventral microsyringe track that spanned the central 2 mm of the BLA. In each subject, this process was repeated sequentially in both hemispheres, resulting in total infusion times of 25 min. Although intra-BLA saline infusions had no effect on striatal LFP activity (*post hoc* paired *t* test, $P = 0.2$; **Fig. 2a**,**c**,**d**), muscimol infusions caused a statistically significant reduction of striatal LFP power that was mostly restricted to gamma activity (paired *t* test, $P = 0.0005$; **Fig. 2b**,**c** and **Supplementary Fig. 7** online).

To examine the relationship between gamma oscillations and unit activity in the BLA and striatum, we constructed peri-event histograms (PEHs) of unit activity around the positive peaks of gamma oscillations recorded by the same microelectrode as the unit activity. To this end, we first isolated gamma by digitally filtering the LFPs and then identified gamma cycles with positive peak exceeding the average plus 2.5 s.d. of the filtered signal (**Fig. 3a**). We then computed histograms of firing for each cell around these reference times. The PEHs give the

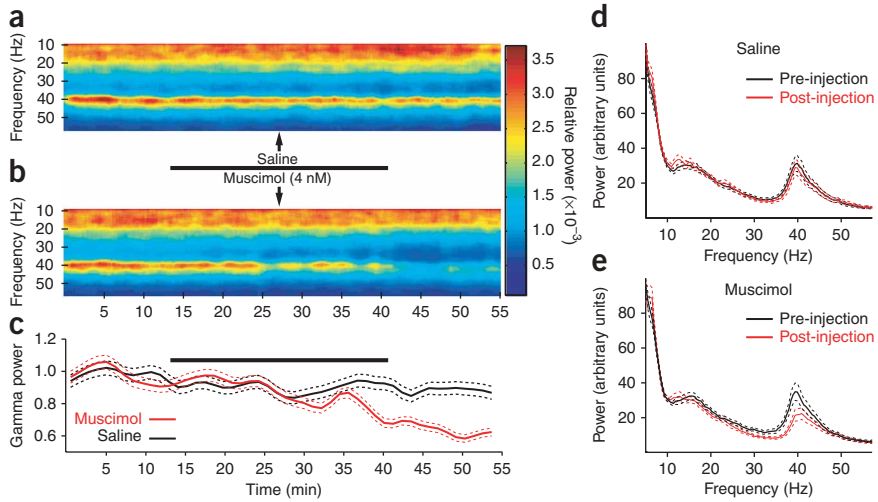

Figure 2 Intra-BLA muscimol infusions reduce striatal gamma power. (**a**,**b**) Striatal LFP power (color coded) at different frequencies plotted as a function of time in experiments in which either saline (**a**) or muscimol (**b**) were slowly infused in the BLA over a period of 25 min. (**c**) Gamma power ± s.e.m. as a function of time when either saline (black) or muscimol (red) were infused in the BLA. In **a**–**c**, the thick black lines indicate the infusion periods. (**d**,**e**) Power spectrum of striatal LFPs during the control (black) and post-infusion (red) phases in experiments in which either saline (**d**) or muscimol (**e**) were infused in the BLA. Dashed lines indicate s.e.m.

To determine whether the gamma modulations of unit activity seen in the PEHs were statistically significant, we computed a rhythmicity index for each cell. The rhythmicity index was obtained by averaging the difference in spike counts between the three center peaks and troughs of the PEHs and dividing the result by the average of the entire histogram to normalize for variations in firing rates. Statistical significance of the rhythmicity index was tested by recomputing the PEHs after shuffling the spike times, repeating this process 1,000 times. The actual rhythmicity index was considered to be significant if it was higher than 95% of the randomly generated rhythmicity indexes ($P < 0.05$). Using this approach, it was determined that the activity of 49% of BLA and 28% of striatal cells was significantly modulated by gamma activity. Next, we examined when BLA and striatal cells fired with respect to gamma activity. To this end, we located the bin with the highest counts in the PEHs and computed a frequency distribution of peak times for each cell with a significant rhythmicity index. This revealed a similar entrainment of BLA and striatal unit activity by local gamma with both cell types firing preferentially during the rising phase of positive gamma cycles (**Fig. 3d**,**e**). The same relation was found for thalamic and cortical units (**Supplementary Fig. 8** online).

impression that BLA (**Fig. 3b**) and striatal cells (**Fig. 3c**) fired repetitively in each gamma burst, but this was not usually the case. In fact, although gamma activity typically occurred in short bursts comprised of 2–6 consecutive high-amplitude cycles, BLA and striatal cells fired infrequently during each burst (BLA, 0.16 ± 0.02 spikes per burst; striatum, 0.18 ± 0.04 spikes per bursts).

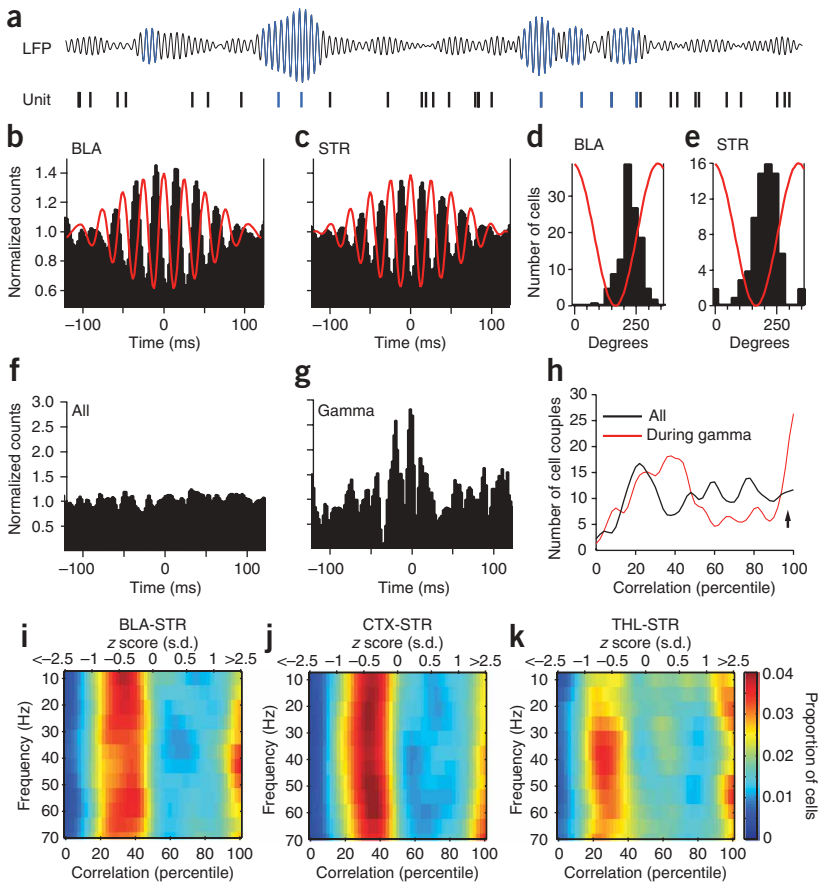

Figure 3 Gamma oscillations increase coupling between the activity of BLA and striatal neurons. (**a**) High-amplitude gamma cycles were detected in the digitally filtered LFPs and PEHs of unit activity were constructed around them. (**b**,**c**) Example of PEHs of BLA (**b**) and striatal (**c**) unit activity around the positive peaks of high-amplitude gamma cycles. To facilitate comparisons between PEHs, we normalized the data to the average bin value. (**d**,**e**) Frequency distributions of firing peak times for BLA (**d**) and striatal (**e**) neurons in relation to gamma. (**f**) Example of a cross-correlogram that included all of the spikes generated by a simultaneously recorded couple of BLA and striatal neurons. (**g**) Cross-correlogram of unit activity for the same cell couple after excluding striatal spikes occurring during periods of low-amplitude gamma. (**h**) Frequency distribution of correlation indices in the cross-correlograms of all BLA-striatal cell couples (black, all spikes; red, analysis restricted to striatal spikes occurring during high-amplitude striatal gamma). (**i**–**k**) Color-coded frequency distributions of correlation indices (*x* axis) plotted as a function of the frequency of striatal LFPs (*y* axis) used to select spikes included in the cross-correlograms. The bottom *x* axis expresses the data in percentiles. The correspondence in *z* scores can be found in the top *x* axis. This was done for all simultaneously recorded couples of BLA and striatal (**i**), cortical and striatal (**j**), or thalamic and striatal (**k**) neurons.

To test whether gamma activity affected functional coupling between BLA and striatal neurons, we examined how LFP power in different frequency bands affected the correlation between striatal and BLA unit activity. To this end, we first cross-correlated unit activity in 362 pairs of simultaneously recorded BLA and striatal neurons. With rare exceptions, these cross-correlograms were flat (**Fig. 3f**). However, when we excluded striatal spikes occurring during periods of low (<2.5 s.d.) gamma power, many cross-correlograms showed significant ($P < 0.05$) coupling (**Fig. 3g**). We assessed the significance of the correlograms by shuffling each of the BLA spike trains 1,000 times, recomputing the correlogram each time and comparing the actual correlogram to the randomly generated values. A correlogram was considered to be significant when the sum of its central bins (±5 ms from origin) was higher than that in 95% of the randomly generated correlograms ($P < 0.05$). To quantify how the incidence of significant BLA-striatal correlations changed in relation to gamma activity, each cell couple was assigned a correlation index (by comparing the sum of the central ±5-ms bins of the correlograms to that of the randomly generated correlograms). The correlation indexes were then rank ordered from the lowest to the highest and expressed as percentiles (**Fig. 3h**). The proportion of correlograms with central bins ≥2.5 s.d. was 15% during high-amplitude gamma, compared with 8% when all spikes were considered. To determine whether this was statistically significant, we performed a χ^2 test analysis comparing the incidence of cell couples with central cross-correlogram peaks higher than versus lower than 2.5 s.d. when all spikes were included versus only those occurring during periods of high-amplitude striatal gamma. The difference was significant ($P = 0.0042$).

To test whether this enhancement of BLA-striatal unit coupling was selective to gamma-related activity, we repeated this analysis in various frequency bands by digitally filtering LFPs in sliding windows of 5 Hz. Using this approach, we observed that significant increases in BLA-unit coupling preferentially occurred in relation to gamma activity (χ^2 test, $P = 0.0042$; **Fig. 3i**). Moreover, when the same analysis was repeated for all available couples of simultaneously recorded cortical and striatal cells ($n = 298$; **Fig. 3j**) or thalamic and striatal ($n = 82$; **Fig. 3k**) neurons, this enhancement of unit correlations by gamma activity was found to be selective for BLA-striatal activity (χ^2 test; corticostriatal, $P = 0.88$; thalamostriatal, $P = 0.29$). Carrying out the same analysis for cortical and BLA or thalamic and BLA cell couples failed to reveal a facilitation of unit coupling by gamma activity (**Supplementary Fig. 9** online).

To determine whether the increased BLA-striatal coupling revealed above was a result of increased discharge rates, we compared baseline firing rates to those seen during periods of high gamma power (>2.5 s.d.). However, increases in gamma power were not associated with changes in the firing rates of BLA (percent change from low to high gamma of 3.2 ± 8.7%, paired t test, $P = 0.14$) or striatal (14.4 ± 19.6%, paired t test, $P = 0.41$) neurons.

Overall, these results suggest that BLA neurons impose gamma activity on the striatum and that functional coupling between BLA and striatal cells is highest during periods of high-amplitude gamma. Thus, coherent striatal and BLA gamma LFP activity is a physiological signature of amygdalostriatal interactions. Notably, this increased coupling of BLA and striatal activity by gamma was not associated with changes in firing rates.

Amygdalostriatal interactions during learning

To investigate whether gamma oscillations also coordinate amygdalostriatal interactions during learning, we trained cats on a stimulus-response task. Memory formation on such tasks is striatal dependent (reviewed in ref. 15). In our case (**Fig. 4a**), cats that had restricted access to food gradually learned that the termination of one of two tones (conditioned stimulus, 3 s) coincided with the brief availability (1 s) of a liquid food reward.

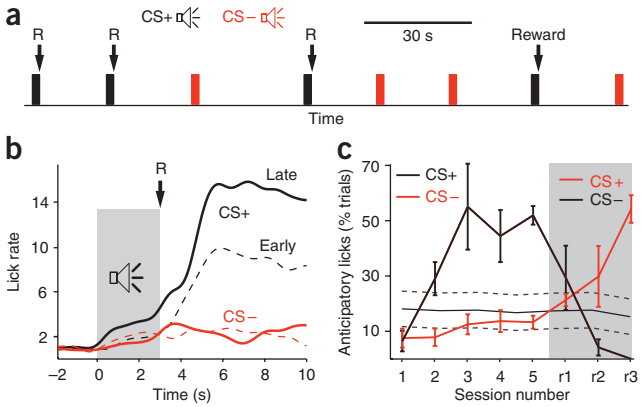

Figure 4 Progression of licking behavior during training on the stimulus-response task. (**a**) The animals were presented with two tones, one unrewarded (CS–, red) and one rewarded (CS+, black), in random order and with variable intertone intervals (20–40 s). The termination of the CS+ coincided with the delivery of a liquid reward (R). (**b**) Normalized licking frequency plotted as a function of time around the tone presentations (gray shading) at early (dashed line) and late (solid line) stages of learning (CS+, black; CS–, red). (**c**) Percent trials with anticipatory licks during the CS+ (black) and CS– (red) plotted as a function of daily training sessions (sessions 1–5). Starting from session r1 (gray shaded area), the tone-reward contingencies were reversed. The gray line indicates spontaneous licking ± s.e.m.

Each daily training session, the cats received around 60 randomly interspersed presentations of the rewarded and unrewarded tones with variable intertrial intervals (range of 20–40 s). Five consecutive daily training sessions occurred with the same rewarded tone before switching reinforcement contingencies. Learning progression was assessed by measuring the rate of anticipatory licking during the rewarded and unrewarded tones, before reward delivery (see Methods).

We determined the licking rate around the rewarded and unrewarded tones during trials obtained during the first and last two training sessions (averaged across all cats; **Fig. 4b**). Although the rate of anticipatory licking during the two tones did not differ significantly at early stages of training (sessions 1–2, $F_{1,\ 1,431} = 0.252$, $P = 0.615$), the difference became significant at late training stages (sessions 4–5, $F_{1,\ 967} = 9.8$, $P = 0.0018$). Plotting the proportion of rewarded and unrewarded tone trials with anticipatory licking as a function of daily training sessions (**Fig. 4c**) revealed that the difference between the rewarded tone, unrewarded tone and spontaneous licking reached statistical significance at the third training session ($F_{2,\ 890} = 11.6$, $P < 0.0001$).

Previous studies using stimulus-response tasks have revealed that BLA unit activity encodes expected outcomes[17–20]. Consistent with the idea that this information is used during learning, it has been reported that BLA-lesioned rats are impaired at associating reward values to specific stimuli in a similar stimulus-response task[21]. Moreover, it has been shown that BLA is required for cue-evoked excitation of nucleus accumbens neurons[22]. These results suggest that BLA might bring an emotional or motivational component to striatal processing during learning.

Consistent with this, we observed a strong parallel between improvements in behavioral performance and correlated amygdalostriatal

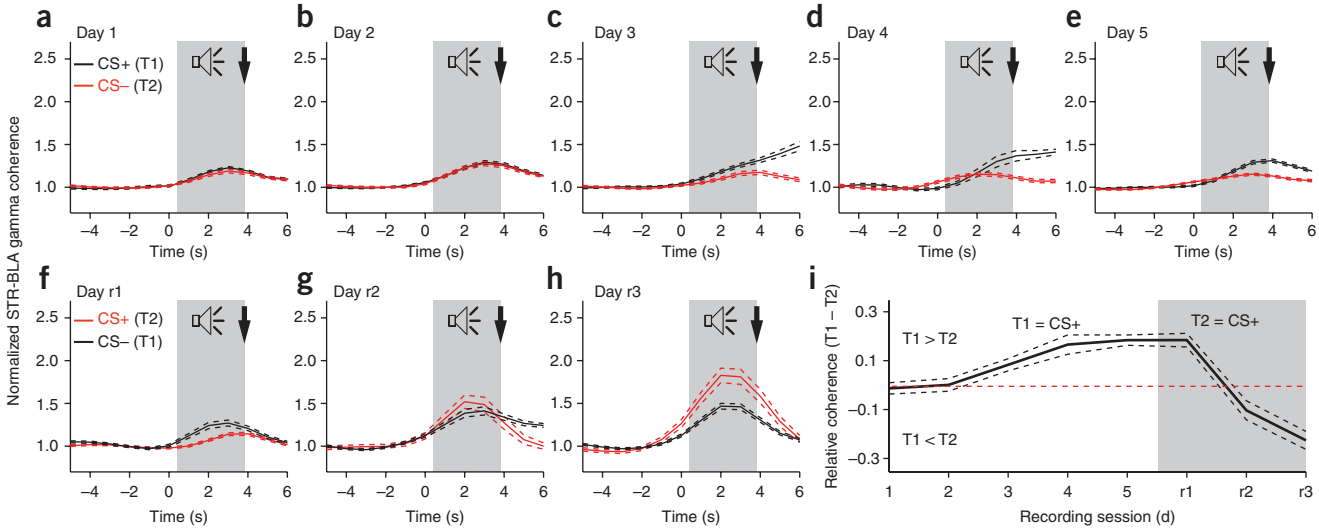

Figure 5 Learning-related changes in correlated amygdalostriatal gamma. Striatal and BLA gamma power was calculated in 1-s windows around tone onset. Striatal-BLA gamma coherence was estimated by computing the product of the BLA and striatal gamma power individually for each 1-s time window. (**a**–**h**) Coherence versus time around onset of CS+ (black lines) and CS– (red lines) ± s.e.m. (dashed lines). Two tone-reward contingences were used: the first between training days 1–5 (**a**–**e**) and the second, where the identities of the CS+ and CS– were reversed, between days r1–3 (**f**–**h**). (**i**) Difference in gamma coherence between the two tones as a function of recording sessions.

gamma during the acquisition of this task ($F_{1,10} = 6.072$, $P = 0.0334$; **Fig. 5**). Early in training (**Fig. 5a**,**b**), the rewarded and unrewarded tones elicited a modest, but significant increase in coherent BLA-striatal gamma (paired *t* test, $P = 0.005$; see **Supplementary Methods** online). However, at this initial stage of training, the increase in coherent BLA-striatal gamma elicited by the two tones were statistically indistinguishable (paired *t* test, days 1–2, $P = 0.72$). As learning progressed, the CS-related BLA-striatal gamma coupling augmented and became significantly more important in response to the rewarded tone (paired *t* test, days 1–2 versus days 3–5, $P = 0.002$; *t* test, rewarded tone versus unrewarded tone on days 3–5, $P = 0.0001$; **Fig. 5c–e**). Notably, the first training session in which the rewarded tone elicited significantly larger increases ($P < 0.05$) in coherent amygdalostriatal gamma activity than the unrewarded tone (day 3; **Fig. 5c**) coincided with the training session in which behavioral evidence of discrimination between the rewarded and unrewarded tones became maximal (day 3; **Fig. 4c**). Moreover, when the reinforcement contingencies were reversed (**Fig. 5f–h**), the identity of the CS eliciting larger increases in coherent BLA-striatal gamma switched and the time course of this effect again paralleled the evolution of behavioral improvements (compare **Figs. 5i** and **4c**).

Further supporting the notion that increases in coherent BLA-striatal gamma are closely related to learning on this task, we found a significant positive correlation between the proportion of trials with anticipatory licking in a given session versus the difference in coherent BLA-striatal gamma elicited by the two tones in the same session ($r = 0.55$, $P < 0.01$; **Fig. 6a**). Yet, the increase in coherent BLA-striatal gamma was not a simple motor correlate, as trials with versus trials without anticipatory licking did not differ in this respect (**Fig. 6b**). Notably, learning-related changes in correlated gamma were only seen between BLA and striatal recording sites, not between striatal and cortical or striatal and thalamic sites (**Supplementary Fig. 10** online). Moreover, examination of learning related fluctuations in other frequency bands that increase coupling between striatal and cortical or thalamic units (**Fig. 3j**,**k**) failed to reveal significant changes ($P \geq 0.4$; **Supplementary Fig. 10**).

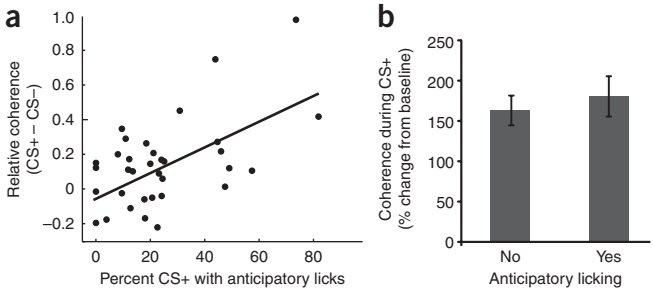

Figure 6 CS+-evoked increases in coherent BLA-striatal gamma parallel behavioral performance, but are not caused by motor outputs. (**a**) Relationship between coherence of BLA-striatal gamma and proportion of CS+ trials with anticipatory licking. Coherence values are relative (CS+ – CS–). Each data point represents a training session. A significant correlation was found ($r = 0.55$, $P < 0.01$). The correlation remained significant ($r = 0.37$, $P < 0.05$) even when the two top-most data points were excluded from the analysis. (**b**) Percent change in BLA-striatal gamma coherence during trials without (left) or with (right) anticipatory licking during the CS+. The difference was not significant (*t* test, $P = 0.58$).

DISCUSSION

This study aimed to shed light on amygdalostriatal interactions during memory formation. The interest of this question stems from pharmaco-behavioral studies implicating BLA activity in the facilitation of striatal-dependent memories by emotional arousal. Our results indicate that gamma oscillations originating in the BLA coordinate amygdalostriatal interactions. Indeed, not only were BLA and striatal LFPs most coherent in the gamma range, but these fast oscillations greatly facilitated coupling of BLA and striatal firing, more so than oscillations in other frequency bands. Moreover, during the acquisition of a striatal-dependent stimulus-response task, the coherence of CS-evoked BLA-striatal gamma increased in parallel with improvements in behavioral performance.

Striatal contributions to memory

Beginning in the 1960s, several studies showed that striatal lesions interfere with the acquisition of various learning tasks (reviewed in refs. 15,23,24). However, because such lesions might have impaired non-mnemonic functions, it remained unclear whether the striatum participated in memory formation. Evidence in support of this role came from studies in which striatal activity was manipulated right after training by performing local drug infusions. For example, long-term striatal-dependent memories can be enhanced by immediate post-training injections of amphetamines and dopaminergic or muscarinic receptor agonists[25–29]. Moreover, intra-striatal infusions of NMDA receptor antagonists immediately after training on a striatal-dependent task interfere with memory[30,31], but not at longer delays. These observations strongly suggest that the striatum is not only required for performance, but is a critical site for memory formation and/or storage[23,24].

Additional evidence for a role of the striatum in memory, independent of its contribution to motor control, came from lesion studies that used pairs of learning tasks sharing the same motivational, sensory and motor features, but in which performance relied on different strategies and cerebral networks. In one study[32], rats could learn the location of a submerged platform in a water maze by either remembering the location of the platform or that of a cue indicating where the platform was located. Striatal lesions selectively interfered with performance in the cued-version of the task, whereas fornix lesions interfered with its spatial version.

Facilitation of striatal memory formation by BLA activity

A large body of evidence indicates that BLA activity facilitates memory in a variety of learning tasks in which memory formation depends on different networks[2]. In one study[13], immediate post-training infusions of amphetamines locally in the BLA facilitated memory formation for the cued (striatal dependent) and spatial (hippocampal dependent) versions of the task. In contrast, infusing lidocaine in the BLA shortly before testing long-term recall had no effect on either task[13], indicating that the BLA is not the storage site of the facilitated memory, but that it is involved transiently during and/or shortly after training to facilitate memory formation in the striatum and hippocampal formation.

Consistent with these observations, BLA activity was also shown to facilitate the induction of activity-dependent synaptic plasticity in a variety of structures, some of which are not directly connected to the BLA. For example, BLA stimulation after LTP induction can enhance and stabilize LTP of perforant path inputs to the dentate gyrus[33–35] and thalamic inputs to the visual cortex[36].

How do BLA inputs facilitate memory formation and synaptic plasticity? The available evidence suggests that multiple parallel mechanisms are involved. One contributing factor resides in the ability of the amygdala to recruit basal forebrain cholinergic neurons that project to the cerebral cortex, resulting in facilitated synaptic plasticity in cortical networks (reviewed in ref. 37). This would explain how BLA stimulation facilitates activity-dependent synaptic plasticity in structures that, in rodents and felines, are devoid of BLA inputs, such as the visual cortex[36] and dentate gyrus[33–35]. In support of this, it has been reported that muscarinic receptor blockade interferes with the stabilizing and facilitating effects of BLA stimulation on LTP of thalamocortical[36] and perforant path[34] inputs. However, as the striatum receives little if any inputs from the basal forebrain[38], another mechanism must be involved.

Consistent with this, we reported previously that the NMDA-to-AMPA ratio is nearly twice as high at BLA inputs as compared with cortical synapses onto principal striatal neurons and that coactivation of BLA and cortical inputs greatly facilitates LTP induction at corticostriatal synapses[14]. Moreover, by selectively blocking NMDA receptors at BLA or cortical synapses onto principal striatal neurons, we showed that NMDA receptor activation at BLA inputs was required for the facilitation of corticostriatal LTP by BLA stimulation[14]. However, the facilitation of corticostriatal LTP by BLA activity that was observed in our previous *in vitro* study required that BLA and cortical inputs coincide with firing of the postsynaptic cell, triggered by injection of large depolarizing currents. As a result, it has been unclear how natural activity patterns could bring about such levels of depolarization.

Gamma as a substrate of amygdalostriatal interactions

Our results shed light on this question by showing that BLA neurons generate periods of gamma activity in the striatum. Indeed, the fact that intra-BLA muscimol infusions caused a selective decrease in striatal gamma constitutes strong evidence that it was generated in the BLA and not by a common input to the BLA and striatum. Moreover, coupling between BLA and striatal unit activity was selectively increased during periods of high striatal gamma. The depolarization of medium spiny neurons that was produced by the arrival of BLA inputs at the gamma frequency probably contributes to enhance NMDA receptor activation and calcium influx in medium spiny neurons, thereby facilitating induction of heterosynaptic activity-dependent plasticity, as recently described *in vitro*[14].

Consistent with this, we also found a close temporal relationship between coherent amygdalostriatal gamma and striatal-dependent learning. Indeed, the emergence of tone-specific coherent amygdalostriatal gamma activity occurred during the same training session as when behavioral evidence of discrimination first reached significance. Notably, evidence that gamma activity generated in the BLA contributes to the induction of learning-related synaptic plasticity was also obtained in other targets of the BLA. For example, it was reported that during the acquisition of an appetitive trace-conditioning task, which is thought to be dependent on the hippocampus, the CS gradually acquired the ability to evoke coherent gamma oscillations in the BLA and rhinal cortices[39] and that this effect contributed to enhance rhinal transfer of neocortical inputs to the hippocampus[40,41]. Together with these earlier studies, our data suggest that the amygdala-mediated facilitation of memory depends on the ability of the BLA to generate gamma oscillations that facilitate the induction of activity-dependent synaptic plasticity in target neurons.

METHODS

Methods and any associated references are available in the online version of the paper at http://www.nature.com/natureneuroscience/.

Note: Supplementary information is available on the Nature Neuroscience website.

ACKNOWLEDGMENTS

This work was supported by a National Institute of Mental Health grant (RO1 MH073610) to D.Paré

Published online at http://www.nature.com/natureneuroscience/
Reprints and permissions information is available online at http://npg.nature.com/reprintsandpermissions/

1. Christianson, S.A. *Handbook of Emotion and Memory: Current Research and Theory* (Erlbaum, Hillsdale, New Jersey, 1992).
2. McGaugh, J.L. The amygdala modulates the consolidation of memories of emotionally arousing experiences. *Annu. Rev. Neurosci.* **27**, 1–28 (2004).
3. Belova, M.A., Paton, J.J., Morrison, S.E. & Salzman, C.D. Expectation modulates neural responses to pleasant and aversive stimuli in primate amygdala. *Neuron* **55**, 970–984 (2007).

4. Pelletier, J.G., Likhtik, E., Filali, M. & Pare, D. Lasting increases in basolateral amygdala activity after emotional arousal: implications for facilitated consolidation of emotional memories. *Learn. Mem.* **12**, 96–102 (2005).
5. Cahill, L. & McGaugh, J.L. Mechanisms of emotional arousal and lasting declarative memory. *Trends Neurosci.* **21**, 294–299 (1998).
6. Castellano, C., Brioni, J.D., Nagahara, A.H. & McGaugh, J.L. Post-training systemic and intra-amygdala administration of the GABA-B agonist baclofen impairs retention. *Behav. Neural Biol.* **52**, 170–179 (1989).
7. Izquierdo, I. *et al.* CNQX infused into rat hippocampus or amygdala disrupts the expression of memory of two different tasks. *Behav. Neural Biol.* **59**, 1–4 (1993).
8. Dickinson-Anson, H., Mesches, M.H., Coleman, K. & McGaugh, J.L. Bicuculline administered into the amygdala blocks benzodiazepine-induced amnesia. *Behav. Neural Biol.* **60**, 1–4 (1993).
9. Hatfield, T. & McGaugh, J.L. Norepinephrine infused into the basolateral amygdala post-training enhances retention in a spatial water maze task. *Neurobiol. Learn. Mem.* **71**, 232–239 (1999).
10. Salinas, J.A., Introini-Collison, I.B., Dalmaz, C. & McGaugh, J.L. Post-training intra-amygdala infusions of oxotremorine and propranolol modulate storage of memory for reductions in reward magnitude. *Neurobiol. Learn. Mem.* **68**, 51–59 (1997).
11. LeDoux, J.E. Emotion circuits in the brain. *Annu. Rev. Neurosci.* **23**, 155–184 (2000).
12. Paré, D., Quirk, G.J. & Ledoux, J.E. New vistas on amygdala networks in conditioned fear. *J. Neurophysiol.* **92**, 1–9 (2004).
13. Packard, M.G., Cahill, L. & McGaugh, J.L. Amygdala modulation of hippocampal-dependent and caudate nucleus-dependent memory processes. *Proc. Natl. Acad. Sci. USA* **91**, 8477–8481 (1994).
14. Popescu, A.T., Saghyan, A.A. & Pare, D. NMDA-dependent facilitation of corticostriatal plasticity by the amygdala. *Proc. Natl. Acad. Sci. USA* **104**, 341–346 (2007).
15. Grahn, J.A., Parkinson, J.A. & Owen, A.M. The cognitive functions of the caudate nucleus. *Prog. Neurobiol.* **86**, 141–155 (2008).
16. Paré, D., Smith, Y. & Pare, J.F. Intra-amygdaloid projections of the basolateral and basomedial nuclei in the cat: phaseolus vulgaris-leucoagglutinin anterograde tracing at the light and electron microscopic level. *Neuroscience* **69**, 567–583 (1995).
17. Paton, J.J., Belova, M.A., Morrison, S.E. & Salzman, C.D. The primate amygdala represents the positive and negative value of visual stimuli during learning. *Nature* **439**, 865–870 (2006).
18. Saddoris, M.P., Gallagher, M. & Schoenbaum, G. Rapid associative encoding in basolateral amygdala depends on connections with orbitofrontal cortex. *Neuron* **46**, 321–331 (2005).
19. Schoenbaum, G., Chiba, A.A. & Gallagher, M. Orbitofrontal cortex and basolateral amygdala encode expected outcomes during learning. *Nat. Neurosci.* **1**, 155–159 (1998).
20. Schoenbaum, G., Chiba, A.A. & Gallagher, M. Neural encoding in orbitofrontal cortex and basolateral amygdala during olfactory discrimination learning. *J. Neurosci.* **19**, 1876–1884 (1999).
21. Balleine, B.W., Killcross, A.S. & Dickinson, A. The effect of lesions of the basolateral amygdala on instrumental conditioning. *J. Neurosci.* **23**, 666–675 (2003).
22. Ambroggi, F., Ishikawa, A., Fields, H.L. & Nicola, S.M. Basolateral amygdala neurons facilitate reward-seeking behavior by exciting nucleus accumbens neurons. *Neuron* **59**, 648–661 (2008).
23. Packard, M.G. & Knowlton, B.J. Learning and memory functions of the basal ganglia. *Annu. Rev. Neurosci.* **25**, 563–593 (2002).
24. Yin, H.H. & Knowlton, B.J. The role of the basal ganglia in habit formation. *Nat. Rev. Neurosci.* **7**, 464–476 (2006).
25. Carr, G.D. & White, N.M. The relationship between stereotypy and memory improvement produced by amphetamine. *Psychopharmacology (Berl.)* **82**, 203–209 (1984).
26. Packard, M.G. & Teather, L.A. Post-training estradiol injections enhance memory in ovariectomized rats: cholinergic blockade and synergism. *Neurobiol. Learn. Mem.* **68**, 172–188 (1997).
27. Packard, M.G. & Teather, L.A. Amygdala modulation of multiple memory systems: hippocampus and caudate-putamen. *Neurobiol. Learn. Mem.* **69**, 163–203 (1998).
28. Packard, M.G. & White, N.M. Dissociation of hippocampus and caudate nucleus memory systems by post-training intracerebral injection of dopamine agonists. *Behav. Neurosci.* **105**, 295–306 (1991).
29. Viaud, M.D. & White, N.M. Dissociation of visual and olfactory conditioning in the neostriatum of rats. *Behav. Brain Res.* **32**, 31–42 (1989).
30. Packard, M.G. & Teather, L.A. Double dissociation of hippocampal and dorsal-striatal memory systems by post-training intracerebral injections of 2-amino-5-phosphono-pentanoic acid. *Behav. Neurosci.* **111**, 543–551 (1997).
31. Packard, M.G. & Teather, L.A. Posttraining injections of MK-801 produce a time-dependent impairment of memory in two water-maze tasks. *Neurobiol. Learn. Mem.* **68**, 42–50 (1997).
32. Packard, M.G. & McGaugh, J.L. Double dissociation of fornix and caudate nucleus lesions on acquisition of two water-maze tasks: further evidence for multiple memory systems. *Behav. Neurosci.* **106**, 439–446 (1992).
33. Akirav, I. & Richter-Levin, G. Biphasic modulation of hippocampal plasticity by behavioral stress and basolateral amygdala stimulation in the rat. *J. Neurosci.* **19**, 10530–10535 (1999).
34. Frey, S., Bergado-Rosado, J., Seidenbecher, T., Pape, H.C. & Frey, J.U. Reinforcement of early long-term potentiation (early-LTP) in dentate gyrus by stimulation of the basolateral amygdala: heterosynaptic induction mechanisms of late-LTP. *J. Neurosci.* **21**, 3697–3703 (2001).
35. Ikegaya, Y., Saito, H. & Abe, K. High-frequency stimulation of the basolateral amygdala facilitates the induction of long-term potentiation in the dentate gyrus in vivo. *Neurosci. Res.* **22**, 203–207 (1995).
36. Dringenberg, H.C., Kuo, M.C. & Tomaszek, S. Stabilization of thalamo-cortical long-term potentiation by the amygdala: cholinergic and transcription-dependent mechanisms. *Eur. J. Neurosci.* **20**, 557–565 (2004).
37. Weinberger, N.M. Specific long-term memory traces in primary auditory cortex. *Nat. Rev. Neurosci.* **5**, 279–290 (2004).
38. Mesulam, M.M., Mash, D., Hersh, L., Bothwell, M. & Geula, C. Cholinergic innervation of the human striatum, globus pallidus, subthalamic nucleus, substantia nigra and red nucleus. *J. Comp. Neurol.* **323**, 252–268 (1992).
39. Bauer, E.P., Paz, R. & Pare, D. Gamma oscillations coordinate amygdalo-rhinal interactions during learning. *J. Neurosci.* **27**, 9369–9379 (2007).
40. Paz, R., Bauer, E.P. & Pare, D. Learning-related facilitation of rhinal interactions by medial prefrontal inputs. *J. Neurosci.* **27**, 6542–6551 (2007).
41. Paz, R., Pelletier, J.G., Bauer, E.P. & Pare, D. Emotional enhancement of memory via amygdala-driven facilitation of rhinal interactions. *Nat. Neurosci.* **9**, 1321–1329 (2006).

ONLINE METHODS

Surgery. Procedures were approved by the Institutional Animal Care and Use Committee of Rutgers University, in compliance with the Guide for the Care and Use of Laboratory Animals (US Department of Health and Human Services). Adult male cats were pre-anesthetized (ketamine, 15 mg per kg of body weight; xylazine, 2 mg per kg, intramuscular) and ventilated with a mixture of ambient air, oxygen and isoflurane. In sterile conditions, an incision was performed on the midline of the scalp and the skull muscles retracted. A reference screw was inserted in the skull overlying the cerebellum and silver-ball electrodes were inserted in the supraorbital cavity to monitor eye movements. Screws were cemented to the skull to later fix the cat's head without pain or pressure. After trepanation and opening of the dura mater, an array of high-impedance tungsten microelectrodes (10–12 MΩ, Frederic Haer) was stereotaxically lowered to the regions of interest (see below). Cats were administered penicillin (20,000 UI per kg of body weight, intramuscular) and an analgesic (ketophen, 2 mg per kg, subcutaneous, daily for 3 d). Recording sessions began 8 d after the surgery.

Recording sites and construction of microelectrode array. The microelectrode array included six electrodes aimed to basal amygdala nuclei, eight electrodes aimed to ventral striatum, eight electrodes aimed to primary or associative auditory cortical areas, and five electrodes aimed to rostral or posterior thalamic intralaminar nuclei. To construct the array, we used a milling machine to drill holes in a Teflon block at stereotaxically defined relative positions. The microelectrodes were then inserted in the holes and their lengths were adjusted such that recordings could be obtained simultaneously from the various recording sites. After cementing the electrodes, the Teflon block was inserted in a tightly fitting Delrin sleeve, which was cemented to the skull. Electrodes could be lowered as a group by means of a micrometric screw.

Recordings. Neuronal activity was sampled at $\geq$100-μm intervals. To insure mechanical stability, we moved the microelectrodes once a day, 30 min before beginning data acquisition. The signals picked up by the electrodes (0.1 Hz to 20 kHz) were observed on an oscilloscope, digitized and stored on a hard disk.

Muscimol injections. To assess the contribution of BLA activity to striatal gamma, we compared the effects of saline versus muscimol infusions in the BLA on striatal gamma power. To this end, we bilaterally implanted two cats with stainless steel guide cannulas aimed at the rostro-caudal center of the BLA under stereotaxic guidance. The cannulas were positioned at the dorsal limit of the BLA, allowing full dorsoventral access for drug infusions. In these cats, we also placed microelectrodes in the striatum, as described above. After a 1-week recovery from the surgery, the animals were gradually adapted to head restraint. During this period, they had restricted access to food, as did the subjects participating in the learning task (see below). Once adapted to head restraint, recording sessions began with a 15-min baseline recording period, after which a total volume of 1 μl per hemisphere of saline or muscimol (4 nM in saline) was infused in the BLA at a rate of 0.08 μl min^{-1}. To this end, a microsyringe with a 25-gauge needle was lowered through the guide cannula and the solution was pressure-injected at ten equidistant sites (0.2-mm spacing) centered on the inner 2 mm of the BLA. The procedure was repeated for the contralateral side and the recording continued for an additional 30 min. In both cats, we carried out two to three saline or muscimol infusions on alternating days.

Behavior. Four cats that had restricted access to food were trained on a stimulus-response task in which the termination of one of two tones (rewarded tone) coincided with the presentation of a liquid food reward (2 ml per trial). The food was available for only 1 s and the cats quickly learned to lick during this interval. The rewarded tone and unrewarded tone tones lasted 3 s and were presented in a random order with 20–40 s intertone intervals. The identity of the rewarded tone and unrewarded tone (3 or 12 kHz) was varied systematically across cats and had no effect on learning progression. Each day, around 60 rewarded tone and 60 unrewarded tone trials were performed. Licking behavior was detected when the cats' tongues interrupted an infrared beam. After five consecutive training sessions, the CS-reward contingencies were reversed. Learning was assessed by monitoring the proportion of rewarded tone and unrewarded tone presentations during which anticipatory licking occurred. In addition, using the 3-s windows preceding tone onsets, we computed the proportion of trials with spontaneous licking for comparison with tone-evoked behavior.

Histology. At the end of the experiments, recording sites were marked with electrolytic lesions (0.5 mA, 5–10 s). The animals were given an overdose of sodium pentobarbital (50 mg per kg, intravenous) and fixed by perfusion. The brains were later sectioned on a vibrating microtome (at 100 μm) and stained with cresyl violet to verify the position of recording electrodes. Microelectrode tracks were reconstructed by combining micrometer readings with the histology.

Data analysis. Data was analyzed offline with custom software written in Matlab 7.1 (MathWorks). Spike-sorting was performed on digitally filtered data (high-pass filter $>$ 150 Hz), using a supervised k-means clustering algorithm. To analyze LFP interactions in specific frequency bands, the raw data was filtered with a 10-Hz bandpass filter, centered on the required frequency (for example, results presented for 40 Hz correspond to data filtered in a 35–45-Hz band). For comparison purposes, all two- and three-dimensional histograms were normalized to the total number of events used. Statistical analyses consisted of repeated measures ANOVAs followed by Bonferonni-corrected *t* tests. All values are reported as average ± s.e.m. To study learning-related fluctuations in BLA-striatal coherence, we calculated the gamma power in 1-s windows (sliding in 100-ms steps) around the onset of the two tones for the two recording sites. Coherence was estimated by computing the product of the powers at the two recoding sites in each window.

doi:10.1038/nn.2305